Free Energy for Protonation Reaction in Lithium-Ion Battery Cathode Materials

R. Benedek,*,† M. M. Thackeray,† and A. van de Walle‡

Chemical Sciences and Engineering Division, Argonne National Laboratory, Argonne, Illinois 60439, and Engineering and Applied Science Division, California Institute of Technology, Pasadena, California 91125

Received October 23, 2007. Revised Manuscript Received May 15, 2008

Calculations are performed of free energies for proton-for-lithium-ion exchange reactions in lithium-ion battery cathode materials. First-principles calculations are employed for the solid phases and tabulated ionization potential and hydration energy data for aqueous ions. Layered structures, spinel $LiMn_2O_4$, and olivine $LiFePO_4$ are considered. Protonation is most favorable energetically in layered systems, such as Li_2MnO_3 and $LiCoO_2$. Less favorable are ion-exchange in spinel $LiMn_2O_4$ and LiV_3O_8. Unfavorable is the substitution of protons for Li in olivine $LiFePO_4$, because of the large distortion of the Fe and P coordination polyhedra. The reaction free energy scales roughly linearly with the volume change in the reaction.

Introduction

Acid treatment of the lithiated transition-metal oxides that are candidate lithium-ion-battery cathode materials has been investigated extensively. Among these materials are lithium−manganese spinel-type materials,[1−7] layered lithium cobaltate,[8−10] and Li_2MnO_3.[11−13] Although Li_2MnO_3 is not itself electrochemically active, acid treatment produces the electrochemically active MnO_2.[13,14] Other applications of acid treatment include battery-material recycling,[15] and ion-sieve material synthesis.[16]

We analyzed previously the free energy of the proton-promoted dissolution and protonation reactions for Li_xCoO_2 in acidic aqueous solution.[17] Dissolution has a lower reaction free energy and is thus thermodynamically favored over the protonation reaction in lithium cobaltate. For other materials, however, such as Li_2MnO_3, protonation is favored, because tetravalent Mn in Li_2MnO_3 is stable against solvation. The reaction energetics of lithiated transition metal oxides can be biased in favor of protonation, relative to dissolution, by increasing the oxidation state of the transition metal ions, while maintaining a concentration of ion-exchangeable lithium. One example of this is the substitution of lithium on the octahedral sites of $LiMn_2O_4$ spinel, which increases the fraction of tetravalent Mn.

The prominence of protonation reactions in the acid treatment of oxides, as well as the relative simplicity of the ion exchange process, make them an attractive subject for analysis. Protonation is simpler than dissolution, for example, because the reaction is expected to have fewer activated steps. Furthermore, free energy calculations for ion exchange are probably more accurate than for dissolution reactions, because of the partial cancelation of errors of corresponding terms in the products and the reactants.[17] Therefore, the absolute values of calculated reaction free energies may be more trustworthy for protonation reactions than for dissolution reactions.

Some protonation reactions are "marginal", in the sense that the calculated protonation free energy is only slightly negative at pH 0, which appears to be the case for $LiMn_2O_4$. At a higher pH, the reaction free energy may reverse sign, with lithiation favored over protonation. The prediction of the crossover pH may be subject to experimental verification, which would provide a direct test of the theoretical analysis.

In this article, we analyze the protonation reaction free energies for $LiMn_2O_4$, Li_2MnO_3, $LiCoO_2$, Li_2NiO_2, LiV_3O_8, and $LiFePO_4$. The protonated forms of some of these materials have previously been the subject of first principles calculations, such as $LiMn_2O_4$.[18] Calculations for nickel

* Corresponding author. E-mail: benedek@anl.gov.
† Argonne National Laboratory.
‡ California Institute of Technology.

(1) Shen, X. M.; Clearfield, A. *J. Solid State Chem.* **1986**, *64*, 270.
(2) Sato, K.; Poojary, D. M.; Clearfield, A.; Kohno, M.; Inoue, Y. *J. Solid State Chem.* **1997**, *131*, 84.
(3) Feng, Q.; Miyai, Y.; Kanoh, H.; Ooi, K. *Langmuir* **1992**, *8*, 1861.
(4) Ammundsen, B.; Jones, D. J.; Roziere, J.; Burns, G. R. *Chem. Mater.* **1995**, *7*, 2151.
(5) Ammundsen, B.; Jones, D. J.; Roziere, J.; Burns, G. R. *Chem. Mater.* **1996**, *8*, 2799.
(6) Ammundsen, B.; Jones, D. J.; Roziere, J.; Berg, H.; Tellgren, R.; Thomas, J. O. *Chem. Mater.* **1998**, *10*, 1680.
(7) Ammundsen, B.; Burns, G. R.; Islam, M. S.; Kanoh, H.; Roziere, J. *J. Phys. Chem. B* **1999**, *103*, 5175.
(8) Zhecheva, E.; Stoyanova, R. *J. Solid State Chem.* **1994**, *109*, 47.
(9) Gupta, R.; Manthiram, A. *J. Solid State Chem.* **1996**, *121*, 483.
(10) Choi, J.; Alvarez, E.; Arunkumar, T. A.; Manthiram, A. *Electrochem. Solid-State Lett.* **2006**, *9*, A241.
(11) Rossouw, M. H.; Thackeray, M. M. *Mater. Res. Bull.* **1991**, *26*, 463.
(12) Rossouw, M. H.; Liles, D. C.; Thackeray, M. M. *J. Solid State Chem.* **1993**, *104*, 464.
(13) Johnson, C. S.; Korte, S. D.; Vaughey, J. T.; Thackeray, M. M.; Bofinger, T. E.; Shao-Horn, T.; Hackney, S. A. *J. Power Sources* **1999**, *81−82*, 491.
(14) Robertson, D.; Bruce, P. G. *Chem. Commun.* **2002**, *23*, 2790.
(15) Shin, S. M.; Kim, N. H.; Sohn, J. S.; Yang, D. H.; Kim, Y. H. *Hydrometallurgy* **2005**, *79*, 172.
(16) Koyanaka, H.; Matsubaya, O.; Koyanaka, Y.; Hatta, N. *J. Electroanalytic Chem.* **2003**, *559*, 77.
(17) Benedek, R.; van de Walle, A. *J. Electrochem. Soc*., in press.
(18) Fang, C. M.; de Wijs, G. A. *Chem. Mater.* **2006**, *18*, 1169.

10.1021/cm703042r CCC: $40.75
Published on Web 08/06/2008

oxyhydroxide have also been performed.[19] We are not aware of previous free energy calculations for protonation reactions, however.

Lithium tends to adopt either octahedral or tetrahedral coordination in oxides. Protons, on the other hand, bond most strongly in a single hydroxyl unit, or in a hydrogen-bonded configuration, in which the proton is bonded to two oxygens. The favorability of the substitution of protons for lithium in lithiated transition metal oxide compounds hinges on the ability of the structure to form a hydroxyl unit without severely degrading the bonding of the rest of the structure by distorting the coordination polyhedra of the transition metal ion (or the phosphate unit in olivine), the network of which forms the backbone of the structure. Our consideration here is restricted to bulk protonation, and the bonding of protons (and hydroxyl units) at defect sites on the anion[7] and transition metal[20] sublattices is not addressed.

An example of a favorable structure for proton substitution is layered Li_2MO_2 (such as with M = Ni) with symmetry $P\bar{3}m1$. The (double) hydroxide $M(OH)_2$ has a similar structure with identical symmetry. If protons are placed on the lithium sites of Li_2MO_2, the protonated system can relax without energy barriers to the hydroxide by translation of the protons parallel to the *c* axis. Another favorable structure for proton substitution is monoclinic Li_2MnO_3,[21] in which the protons substitute for lithium in the pure Li layer. A shear transformation[21] reorders the layer stacking sequence, which results in a structure whose prototype is $HCrO_2$.[22] The stacking of oxygen layers transforms from *ABCABC* to *ABBCCA*. Our calculations indicate that $LiFePO_4$ olivine is unfavorable for proton substitution, because the Fe and P coordination polyhedra must be severely perturbed for the structure to accommodate protons.

We find that the volume of the protonated phase, relative to that of the parent lithiated phase, correlates closely with the reaction free energy. A compact protonated phase, with symmetric and undistorted MO polyhedra, leads to a low reaction free energy.

Methods

The calculations employed the Dudarev et al. formulation[23] of the GGA+U method, as implemented in the VASP code,[24−26] for both the lithiated and the associated proton-substituted materials. On-site Coulomb parameters $U-J = 5$ for Co(3+), 4 for Ni(2+), 4.5 for Mn(3.5+), 4 for Fe(2+), in eV, similar to those obtained by Zhou et al. based on a self-consistency criterion,[27] and $U-J = 2$ for V(5+).[28] The reaction free energies calculated below are actually quite insensitive (change by the order of $1 \times 10^{-2}\ \delta U$) to the precise values of $U-J$ because they involve a difference between energies for lithiated and protonated systems, in which a change in *U* affects both similarly; a slightly higher dependence on *U* would occur if it were different for corresponding protonated and lithiated materials.

The VASP precision level was set at "high", which corresponds to an energy cutoff of 500 eV. Special k-points were employed for Brillouin-zone sampling,[29] with Monkhorst−Pack indices (8,8,8), for the smallest unit cells.

Ferromagnetic spin configurations were assumed for those systems in which transition metal ions had nonzero moments, although more complex magnetic configurations occur in some of the materials, such as $LiMn_2O_4$ at low temperatures. Only fully lithiated or protonated systems are considered. Both the cell parameters and the internal coordinates are optimized in all cases. Coordinates for the lithiated systems were employed as initial (unrelaxed) coordinates for the protonated systems in the case of HMn_2O_4, HV_3O_8 and $HFePO_4$, for which structures are unknown.

Our methodology yields a relaxed configuration and local energy minimum closest to the starting configuration. That substantially lower energy configurations than those obtained in the present work may exist cannot be ruled out without an exhaustive search; however, we believe this is unlikely.

The $Fd\bar{3}m$ symmetry for spinel $LiMn_2O_4$ represents the "average" structure of the material at room temperature, and was assumed in our calculations. We assign a charge of +3.5 to all Mn atoms, to approximately represent the state of the material above its charge ordering temperature. Large charge and spin fluctuations, however, are expected to occur for this system, in view of its mixed valence (mean Mn oxidation state 3.5) and proximity to a transition to an orthorhombic structure (*Fddd* symmetry), accompanied by charge ordering, at 230 K,[30] or at higher temperatures, depending on the oxygen stoichiometric deficiency. These excitations are beyond the scope of the mean-field treatment of the GGA+U method, and therefore give rise to additional uncertainty in calculations for $LiMn_2O_4$ and HMn_2O_4.

Protons placed in tetrahedral sites in HMn_2O_4 are unbonded. If they are displaced slightly along the cubic diagonal axis, however, they relax to form hydroxyl complexes,[18] and the resultant energy is lowered. The configuration of protons is not unique, and several arrangements give fairly comparable energies. The results presented in the tables represent a proton configuration that drives a small trigonal distortion.

When protons are substituted for the Li layers in Li_2MnO_3, a change in the layer stacking sequence occurs, as mentioned above. Calculations for the Li_2MO_3 systems are performed with either an eight-formula-unit (conventional) cell,[31] or the primitive two-formula unit cell. When protons are substituted in the Li layers, the system relaxes to the $HCrO_2$ structure.[22]

Results

We consider the reaction

$$x\mathrm{H}^+(\mathrm{aq}) + \mathrm{Li}_{x+y}\mathrm{M}_z\mathrm{O}_u \rightarrow x\mathrm{Li}^+(\mathrm{aq}) + \mathrm{H}_x\mathrm{Li}_y\mathrm{M}_z\mathrm{O}_u \quad (1)$$

where $y = 0$ in most cases that we treat. In Li_2MnO_3, however, the substitution initially occurs only in the pure Li layer, and not in the mixed Li−Mn layer.

(19) der Ven, V.; Morgan, D.; Meng, Y. S.; Ceder, G. *J. Electrochem. Soc.* **2006**, *153*, A210.
(20) Ruetschi, P. *J. Electrochem. Soc.* **1984**, *131*, 2737.
(21) Paik, Y.; Grey, C. P.; Johnson, C. S.; Kim, J. S.; Thackeray, M. M. *Chem. Mater.* **2002**, *14*, 5109.
(22) Hamilton, W. C.; Ibers, J. A. *J. Solid State Chem.* **1963**, *16*, 1209.
(23) Dudarev, S. L.; Botton, G. A.; Savrasov, S. Y.; Humphreys, C. J.; Sutton, A. P. *Phys. Rev. B* **1998**, *57*, 1505.
(24) Kresse, G.; Furthmueller, J. *Comput. Mater. Sci.* **1996**, *6*, 15.
(25) Kresse, G.; Furthmueller, J. *Phys. Rev. B* **1996**, *54*, 11169.
(26) Kresse, G.; Joubert, D. *Phys. Rev. B* **1999**, *59*, 1758.
(27) Zhou, F.; Cococcioni, C.; Marianetti, C. A.; Morgan, G.; Ceder, G. *Phys. Rev. B* **2004**, *70*, 235121.
(28) Elfimov, I. S.; Saha-Dasgupta, T.; Korotin, M. A. *Phys. Rev. B* **2003**, *68*, 113105.
(29) Monkhorst, J.; Pack, D. *Phys. Rev. B* **1976**, *13*, 5188.
(30) Rousse, G.; Masquelier, C.; Rodriguez-Carvajal, J.; Elkaim, E.; Lauriat, J. P.; Martinez, J. L. *Chem. Mater.* **1999**, *11*, 3629.
(31) Jansen, M.; Hoppe, R. *Z. Anorg. Allg. Chem.* **1973**, *397*, 279.

Table 1. Energy Differences for the Substituted Lithiated Transition-Metal Oxides Relative to the Reference Systems, Along with the Prototype Material for the Protonated System and Its Symmetry[a]

substituted system	prototype	symmetry	reference system	$\Delta E_{(s)}$	ΔG^0
$Ni(OH)_2$	$Mg(OH)_2$	$P\bar{3}m1$	Li_2NiO_2	−0.19	−1.41
$HCoO_2$	$HCrO_2$	$R\bar{3}m$	$LiCoO_2$	0.333	−0.88
$HLi_{1/3}Mn_{2/3}O_2$	$HCrO_2$	$R\bar{3}m$	Li_2MnO_3	0.494	−0.70
$H(H_{1/3}Mn_{2/3})O_2$	$HCrO_2$	$R\bar{3}m$	$HLi_{1/3}Mn_{2/3}O_2$	1.09	−0.14
HMn_2O_4	$MgAl_2O_4$	$Fd\bar{3}m$	$LiMn_2O_4$	0.93	−0.2
HV_3O_8	LiV_3O_8	$P2_1/m$	LiV_3O_8	1.17	−0.04
$HFePO_4$	$LiFePO_4$	*Pnma*	$LiFePO_4$	2.56	1.43

[a] The energy difference ΔE_s, between the proton-substituted system and the reference system, in eV per ion exchange, is given in the fifth column. The sixth column, ΔG^0, is the reaction free energy for proton-for-lithium-ion exchange from an aqueous solution [cf. eq 1].

We express the standard reaction free energy difference (at 1 bar, 298.15 K, pH 0) as

$$\Delta G^0 = \Delta G^0(\mathrm{s}) + \Delta G^0(\mathrm{aq}) \qquad (2)$$

where $\Delta G^0(\mathrm{s}) = G^0(\mathrm{s_p}) - G^0(\mathrm{s_r})$ is the difference between the (proton-exchanged) product phase and the (lithiated) reactant phase free energies of the solid phases, and $\Delta G^0(\mathrm{aq})$ is the difference between the hydration free energy of Li ions and protons. The protonated product phase, s_p, may have a different crystal structure, e.g., with a different stacking sequence in layered systems, from the original compound, s_r. The solid phase contribution, $\Delta G^0(\mathrm{s})$ is divided into an effective cohesive term $\Delta E^0(\mathrm{s})$, which is calculated with the VASP code, and a vibrational contribution $\Delta G_{\mathrm{vib}}(T)$, in which a Born−von Kàrmàn lattice-dynamical analysis is performed, with spring constants determined by a least-squares fit to the reaction forces resulting from imposed displacements in a supercell geometry.[32]

The contribution $\Delta G^0(\mathrm{aq})$ of the aqueous species is the difference $G^0(\mathrm{Li^+}) - G^0(\mathrm{H^+})$, where

$$G^0(\mathrm{Li^+}) = E_{\mathrm{ref}}(\mathrm{Li}) + E_{\mathrm{ion}}(\mathrm{Li}) + G_{\mathrm{hyd}}(\mathrm{Li}) \qquad (3)$$

a similar expression holds for $G^0(\mathrm{H^+})$. $E_{\mathrm{ref}}(\mathrm{aq_i})$ is the neutral atom energy for species $\mathrm{aq_i}$, calculated with the VASP code, relative to an atomic reference energy set by the VASP code (this arbitrary reference energy cancels out in calculations of reaction free energies). We obtain E_{ref} values of −0.27 for Li and −1.12 for H, in eV. The ionization energies are 5.39 for Li and 13.6 for H, in eV. The hydration free energies[33] are −5.49 for Li and −11.45 for H, in eV. The net result is $\Delta G^0(\mathrm{aq}) = -1.42$ eV.

In previous analysis[17] of the reactions of lithium cobaltate in acid, $G_{\mathrm{vib}}(T)$ was evaluated for several hydrogen and lithium bearing layered cobalt oxides with codes developed by one of the authors.[34−36] Vibrational free energy calculations for such oxides, however, can be computationally demanding, for several reasons: (i) low symmetry crystals require a large number of symmetrically distinct displacements to determine the spring constants, (ii) the long-range electrostatic interactions make computationally expensive large supercells unavoidable, and (iii) the shallowness of the energy minima, particularly for H, restrict atomic displacements to small values for which Hellmann−Feynman forces are not well converged. The selection of injudiciously small supercells or large atomic displacements may lead to artifact unstable modes.

As an alternative to explicit calculations of $G_{\mathrm{vib}}(T)$ for Li_2MnO_3 and other low-symmetry systems under consideration in this work, we resort to an approximate formula[17]

$$G_{\mathrm{vib}}(300\mathrm{K}) \approx 0.25\nu(\mathrm{H}) + 0.1\nu(\mathrm{O}) + 0.04\nu(\mathrm{Li}) \qquad (4)$$

in eV per formula unit, where the coefficients $\nu(i)$ are the number of i atoms per formula unit.

Equation 4 closely represents results for $LiCoO_2$, $HCoO_2$, and Co_3O_4 (eq 4: 0.24, 0.45, 0.4; explicit calculation: 0.235, 0.468, 0.421) The transferability of eq 4 was also tested for $LiMn_2O_4$, HMn_2O_4, Mn_2O_4, NiO, H_2NiO_2 and CoO_2 (eq 4: 0.44, 0.65, 0.40, 0.10, 0.70, 0.20; explicit calculation: 0.23, 0.56, 0.36, 0.03, 0.71, 0.07). The largest absolute discrepancy occurs for spinel $LiMn_2O_4$, for which eq 4 overpredicts $G_{\mathrm{vib}}(300\mathrm{K})$ by about a factor of 2, perhaps partly as a result of instabilities of the $Fd\bar{3}m$ structure not far below room temperature.

Application of eq 4 to the vibrational free energy contribution for H−Li ion exchange yields $\Delta G^0_{\mathrm{vib}}(300\ \mathrm{K}) = 0.25 - 0.04 = 0.21$ eV. In the case of spinel, we can check this prediction against explicit lattice dynamical calculations for $LiMn_2O_4$ and HMn_2O_4, which yield $\Delta G^0_{\mathrm{vib}}(300\ \mathrm{K}) = 0.33$ eV. On the basis of this comparison, we estimate that the error introduced in $\Delta G^0_{\mathrm{vib}}(300\ \mathrm{K})$ by the use of eq 4) is therefore on the order of 0.1 eV or less.

Table 1 lists the main results of this work. The first column gives the composition of the protonated system derived from the reference system listed in the fourth column. The prototype system that exemplifies the structure adopted by the protonated system is listed in the second column, and the symmetry of the prototype is listed in the third column. The quantity $\Delta E^0(\mathrm{s})$ is the difference in total energy between the proton-substituted and the reference system, per hydrogen-for-lithium substitution, calculated with the VASP code. The quantity ΔG^0 represents the reaction free energy, per ion exchange, of simultaneously replacing a proton in aqueous solution with a lithium ion while substituting a proton for a lithium atom in the oxide. On the basis of the above analysis

$$\Delta G^0 = \Delta E^0(\mathrm{s}) + \Delta G^0_{\mathrm{vib}}(300\mathrm{K}) + \Delta G^0(\mathrm{aq}) \approx \Delta E^0(\mathrm{s}) - 1.21 \qquad (5)$$

is the reaction free energy, in eV, at pH 0, if we employ eq 4 for the vibrational free energy. Thus, the reaction energy is essentially proportional to $\Delta E^0(\mathrm{s})$, which varies widely with the material, but is shifted downward by a roughly constant value of more than 1 eV.

(32) van de Walle, A; Ceder, G. *Rev. Mod. Phys.* **2002**, *74*, 11.
(33) Fawcett, W. R. *J. Phys. Chem. B* **1999**, *103*, 11181.
(34) van de Walle, A.; Asta, M.; Ceder, G. *CALPHAD* **2002**, *26*, 539.
(35) van de Walle, A.; Ceder, G. *J. Phase Equilib.* **2002**, *23*, 348.
(36) van de Walle, unpublished; see www.its.caltech.edu/avdw/atat/ (2007).

Table 2. Structural Parameters for Reference (Lithiated) Systems and Protonated Systems, Calculated with GGA+U Method[a]

system	*a*	*b*	*c*	z_H	r_{OH}	ΔV
Li_2NiO_2	3.13		5.07			
$Ni(OH)_2$	3.10 (3.126) [38]		4.59 (4.605)	1	0.97	−3.2
$LiCoO_2$	2.83 (2.815) [51]		14.13 (14.05)			
$HCoO_2$	2.86 (2.851) [43]		13.78 (13.15)	2	1.2	−1.5
$Li_2\ MnO_3$	5.01(4.93) [31]	8.67(8.53)	9.60 (9.60)			
$H(Li_{1/3}\ Mn_{2/3})O_2$	8.84		4.43	2	1.1−1.3	−1.5
$H(H_{1/3}Mn_{2/3})O_2$	8.83		4.62	1	1.0	3.7
$LiMn_2O_4$	8.40 (8.24) [52]					
HMn_2O_4	8.22			1	0.99	−3.3
LiV_3O_8	6.78(6.596) [53]	3.66 (3.559)	12.07 (11.862)			
HV_3O_8	6.67	3.68	12.30	1	0.98	2.8
$LiFePO_4$	10.43(10.38) [54]	6.08(6.01)	4.75 (4.72)			
$HFePO_4$	12.79	4.97	5.29	1	1.32	8.5

[a] The systems considered are the same as those listed in Table 1. Calculated lattice constants appear in columns 2−4. z_H is the number of oxygen atoms coordinated with the substituted proton. r_{OH} is the corresponding hydroxyl bond length (or range of bond lengths). The last column is the volume difference between the substituted and reference systems, in cubic angstroms per substitution. Experimental values are in parentheses.

Table 2 lists calculated structural properties of the lithiated and protonated systems, as well as experimentally observed lattice constants (in parentheses). The agreement between calculated and observed lattice constants is of the order of one percent in most cases, which is fairly typical of calculations at the GGA+U level. A notable exception is the overprediction by almost 5% of the *c*-axis lattice constant of $HCoO_2$, which may be associated with dynamical effects of H not included in the calculations.

The quantity z_H in Table 2 is the number of oxygen atoms coordinated with the substituted proton within a distance r_{OH} of about 1.4 Å. The last column gives the volume change, ΔV of the oxide, in cubic angstroms per ion exchange. The proton coordination number, the hydroxyl bond length, and the volume change per ion exchange, are discussed below.

Li_2NiO_2. The overlithiated lithium nickelate may be taken as a prototype system for H−Li ion exchange, in view of the high stability of the hydroxide and the identical space group symmetry of the original and substituted systems. 1T-Li_2NiO_2 may be obtained by the overdischarge of $R\bar{3}m$ $LiNiO_2$, although the ground-state of Li_2NiO_2 is orthorhombic.[37] Both 1T-Li_2NiO_2 and β-$Ni(OH)_2$[38] have symmetry $P\bar{3}m1$. If protons are substituted at the lithium sites of 1T-Li_2NiO_2 and the system is allowed to relax, under the action of the Hellmann−Feynman forces, it transforms, without energy barriers, to $P\bar{3}m1$-$Ni(OH)_2$ by a translation of the protons parallel to the *c*-axis. The ion exchange reaction for this system is the most energetically favorable of all the systems listed in Table 1.

$LiCoO_2$. The oxyhydroxide of Co, i.e., β-$HCoO_2$, may be obtained, for example, by oxidation of the hydroxide,[39] as well as by H−Li ion exchange in $LiCoO_2$ under acidic hydrothermal conditions.[40] (Li−H ion exchange in $HCoO_2$ occurs under appropriate basic hydrothermal conditions.[41,42]) Like $LiCoO_2$, $HCoO_2$ has $R\bar{3}m$ symmetry, however, the stacking sequence of the oxygen sublattice is shifted, with little if any energy barrier, to *ABBCCA*, to enable hydrogen to bond to oxygen in layers both above and below it.[43] Calculations suggest that the hydrogen atoms experience a double-well potential, with a potential maximum halfway between a pair of oxygen atoms, at distance of about 1.22 Å from each, and minima offset by 0.15 Å toward either of the oxygens. Because of the shallowness of the minima, the protons oscillate between them, and, in effect, each minimum has an occupancy of 0.5. Early neutron diffraction experiments[43] detected asymmetry in the site occupancies for deuterated but not hydrogen-bearing specimens. Later work on the isomorphous system,[44] $HCrO_2$, revealed an off-center and disordered hydrogen configuration. In principle, an additional contribution kT ln 2 should be added to the free energy to account for the configurational entropy in the case of a shallow double-well potential, however this would only minimally shift the numerical results listed in the tables.

Li_2MnO_3. The electrochemically inert layered defect-rocksalt compound Li_2MnO_3 has been structurally integrated with more electrochemically active layered compounds in order to enhance Li-ion-battery cathode stability.[45,46] It is also under consideration as an oxygen reduction catalyst.[47] Proton exchange reactions are expected to be favorable in this material, relative to dissolution, because the high oxidation state of the transition metal effectively prevents its dissolution, although leaching of Li_2O to produce MnO_2[13,14] is possible.

Cation layers of Li_2MnO_3 are of two types, pure Li and $Li_{1/3}Mn_{2/3}$. The driving force for ion exchange in the Li layers, by the reaction

$$H^+ + Li(Li_{1/3}Mn_{2/3})O_2 \rightarrow Li^+ + H(Li_{1/3}Mn_{2/3})O_2 \quad (6)$$

is relatively large, as seen in Table 1. The substitution of protons on the Li sites in Li_2MnO_3 is accompanied by a shear

(37) Kang, C. H.; Chen, B. J.; Huang, G.; Ceder, *Chem. Mater.* **2004**, *16*, 2685.
(38) Dittrich, H.; Axmann, P.; Wohlfahrt-Mehrens, M.; Garche, J.; Albrecht, S.; Meese-Marktscheffel, J.; Olbrich, A.; Gille, G. *Z. Kristallogr.* **2005**, *220*, 306.
(39) Butel, M.; Gautier, L.; Delmas, C. *Solid State Ionics* **1999**, *122*, 271.
(40) Fernandez-Rodriguez, J. M.; Hernan, L.; Morales, J.; Tirado, J. L. *Mater. Res. Bull.* **1988**, *23*, 899.
(41) Larcher, D.; Palacin, M. R.; Amatucci, G. G.; Tarascon, J. M. *J. Electrochem. Soc.* **1997**, *144*, 408.
(42) Tao, Y.; Zhu, B.; Chen, Z. *J. Alloys Compd.* **2007**, *430*, 222.
(43) Delaplane, R. G.; Ibers, J. A.; Ferraro, J. R.; Rush, J. J. *J. Chem. Phys.* **1969**, *50*, 1920.
(44) Ichikawa, M.; Gustafsson, T.; Olovsson, I.; Tsuchida, T. *J. Phys. Chem. Solids* **1999**, *60*, 1875.
(45) Johnson, S.; Kim, J. S.; Lefief, C.; Li, N.; Vaughey, J. T.; Thackeray, M. M. *Electrochem. Commun.* **2004**, *6*, 1085.
(46) Thackeray, M.; Johnson, C. S.; Vaughey, J. T.; Li, N.; Hackney, S. A. *J. Mater. Chem.* **2005**, *15*, 2257.
(47) Ngala, J. K.; Alia, S.; Dobley, A.; Crisostomo, V. M. B.; Suib, S. L. *Chem. Mater.* **2007**, *19*, 229.

transformation,[45] similar to that for protonated $LiCoO_2$, whereby the layer stacking sequence transforms to that of the $HCrO_2$ structure.

That this transformation is essentially without barrier can be demonstrated by a simulation in which a starting configuration with H substituted for Li in the Li layers of monoclinic Li_2MnO_3 is relaxed to achieve an energy minimum, by a steepest-descents-like approach. The energy, structure, and bond lengths for the relaxed structure are essentially identical to those for hexagonal $H(Li_{1/3}Mn_{2/3})O_2$ in the $HCrO_2$ structure. This calculation suggests that barriers to the transformation from the original monoclinic structure with $C2/c$ symmetry to the hexagonal structure with symmetry $R\bar{3}m$ are small.

The results in the Table indicate that substitution of the remaining Li atoms in $HLi_{1/3}Mn_{2/3}O_2$ with protons

$$H^+ + 3H(Li_{1/3}Mn_{2/3})O_2 \rightarrow Li^+ + 3H_{4/3}Mn_{2/3}O_2 \qquad (7)$$

is still energetically favorable, but considerably less so than reaction 6. Experiment[47] has shown that at least partial substitution of H for Li in the LiMn layers is possible.

$LiMn_2O_4$. A nonlayered structure of interest is the cubic spinel $LiMn_2O_4$, for which VASP calculations at the GGA level of proton substitution have recently been presented.[18] A significant feature is the unique value of the hydroxyl bond length r_{OH} of about 1.0 Å for protons that substitute for Li on 8*a* sites. The larger value of 1.1 Å obtained from neutron scattering measurement refinements,[4,6] may be at least partly related to the $Fd3m$ symmetry assumed in the refinement, as previously noted.[18] Another complication, is the effect of charge and spin fluctuations at room temperature, mentioned above, not included in our free energy calculations.

Our calculations (cf. Table 1) suggest that there is a small driving force, about −0.2 eV, to protonate lithium manganese spinel, at pH 0. If this prediction were taken at face value, the reaction free energy would go through zero at approximately pH 3.5, with lithiation being favored at higher pH and protonation at lower pH. In $LiMn_2O_4$; however, these ion-exchange reactions are likely masked by the spinel dissolution reaction.[48] By substitution of Li on the Mn sublattice of $LiMn_2O_4$, the driving force for dissolution is suppressed, and overlithiated systems near the composition $Li_4Mn_5O_{12}$ may be more suitable for investigation of the competition between protonation and lithiation reactions than stoichiometric $LiMn_2O_4$ spinel.

LiV_3O_8, $LiFePO_4$. These systems, particularly olivine, exemplify structures in which protonation is relatively unfavorable. The accommodation of protons in $HFePO_4$, for example, would require severe distortion of the Fe octahedra and P tetrahedra. Furthermore, even with these large distortions, the hydroxyl bond length (cf. Table 2) is still much larger than in favorable situations. Our results are consistent with recent experimental work,[10] which showed essentially no hydrogen absorption into $FePO_4$.

Discussion

Proton-for-lithium ion-exchange is found most favorable in layered systems with close-packed layers in which the oxygen sublattice exhibits either cubic or hexagonal stacking. Simulations further suggest that the barriers to the stacking rearrangements necessary to accommodate substituted protons in Li_2MnO_3 (or $LiCoO_2$) are small or negligible. Protonation of the cubic spinel $LiMn_2O_4$ is less favorable than in the layered structures, and protonation of the trivanadate LiV_3O_8, and particularly $LiFePO_4$ olivine, is least favorable.

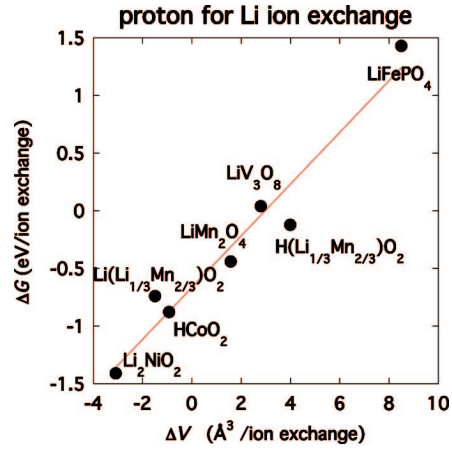

Figure 1. Standard reaction free energy for the exchange of protons for Li, versus volume change (difference between volume of protonated and lithiated systems).

Protonated and lithiated systems are most "compatible" if the transition-metal-oxide framework structure can form strong hydroxyl bonds without a severe distortion of the MO host polyhedra, when protons are substituted for lithium ions. Layered systems possess such compatibility, since they can adapt to proton-for-lithium substitution by adjustment of the interlayer spacing and by the sliding of layers relative to each other, without severe perturbation to the metal-oxide octahedra. On the other hand, host structures in which the lithium ions are organized in channels, such as $LiMn_2O_4$, as well as systems with disparate metal-oxide polyhedra, such as LiV_3O_8 and olivine $LiFePO_4$, do not have this freedom, and therefore have lower proton−lithium compatiblity.

A close correlation exists between the reaction free energy and the volume change ΔV per ion exchange, as shown in Figure 1. The data follow an approximately linear dependence

$$\Delta G^0 = -0.67 + 0.22\Delta V \qquad (8)$$

in eV per ion exchange, where volume is in $Å^3$. Structures in which protons are accommodated compactly, with small distortion to the transition-metal polyhedra, have relatively low ΔV, and are thus energetically favorable.

The correlation between thermodynamic properties and volume change induced by proton substitution in oxides appears not to have been discussed previously. The correlation of hydrogen partial molar volumes with other thermodynamic properties is well-known in the context of metal alloys.[49] Because interstitial protons in metal alloys are essentially nonbonded, however, maximum spacing from nearest neighbor metal atoms is energetically preferred. A

(48) Hunter, J. C. *J. Solid State Chem.* **1981**, *39*, 142.

(49) Lindsay, W. T. *Int. J. Thermophys.* **1997**, *18*, 1051.

negative value of $\partial\Delta G_H/\partial V_H$, contrary to eq 8, is found for hydrogen absorption from the gas phase, where the partial volume of the interstitial hydrogen, V_H varies as a function of alloy composition, e.g., $Pd_{1-x}Ag_x$.[49] The physics of hydrogen in metals in therefore in strong contrast to that in oxides, in which the protons occupy lattice sites and bond to nearest neighbor oxygen atoms.

For most of the materials investigated in this work, protons bond to a single oxygen, $z_{OH} = 1$, with a hydroxyl bond length of about 1 Å. The $HCrO_2$ structure,[50] adopted by HCo_2, has one oxygen above and one below each proton, along the *c* axis, and thus $z_{OH} = 2$. For this system, the proton experiences a double-well potential, and favors a slightly off-centered position.[17] The most stable site for a proton in spinel is displaced from the 8*a* site toward one of the oxygen ions that comprise the surrounding tetrahedral cage of 16*d* sites.[18]

Conclusion

The calculated standard reaction free energies ΔG^0 for proton-for-lithium ion exchange in lithiated-transition-metal oxides confirm that structures based on close packed layers are most favorable for such reactions. Such systems have the flexibility to accommodate bonding of either lithium or proton layers, without severe distortion of the metal oxide octahedra, by adjustment of the interlayer spacings and/or by the sliding of the layers relative to each other, i.e., a change in the stacking sequence. Lithium−proton compatibility is lower in structures based on one-dimensional channels of lithium ions, or structures in which multiple (more than one) metal-oxide polyhedra coexist in the lithiated system, because host polyhedra cannot avoid appreciable distortion when protons are substituted for lithium. Reaction energies ΔG^0 are predicted to vary essentially linearly with volume change per ion exchange.

Acknowledgment. The submitted manuscript has been created by UChicago Argonne, LLC, Operator of Argonne National Laboratory (″Argonne″). Argonne, a U.S. Department of Energy Office of Science laboratory, is operated under Contract No. DE-AC02-06CH11357. This work was supported at Argonne by the Office of FreedomCar and Vehicle Technologies (Batteries for Advanced Transportation Technologies (BATT) Program), U.S. Department of Energy. A.v.d.W. was supported by the National Science Foundation through TeraGrid computing resources provided by NCSA and SDSC under grant DMR060011N. Grants of computer time at the National Energy Research Supercomputer Center, Lawrence Berkeley Laboratory are gratefully acknowledged.

CM703042R

(50) Hamilton, W. C.; Ibers, J. A. *Acta Crystallogr.* **1969**, *16*, 1209.
(51) Amatucci, G. G.; Tarascon, J. M.; Klein, L. C. *J. Electrochem. Soc.* **1996**, *143*, 1114.
(52) Masquelier, M.; Tabuchi, K.; Ado, R.; Kanno, Y.; Kobayashi, Y.; Maki, O.; Nakamura, J. B.; Goodenough, *J. Solid State Chem.* **1996**, *123*, 255.
(53) de Picciotto, L. A.; Adendorff, K. T.; Liles, D. C.; Thackeray, M. M. *Solid State Ionics* **1993**, *62*, 297.
(54) Yang, S.; Zavalij, P. Y.; Whittingham, M. S. *Electrochem. Commun.* **2001**, *3*, 505.